INVITED PAPER *Special Section on Recent Advances in Integrated Photonic Devices*

Optical Microsensors Integration Technologies for Biomedical Applications

Eiji HIGURASHI[†a)], ***Member***, **Renshi SAWADA**[††], ***and*** **Tadatomo SUGA**[†], ***Nonmembers***

SUMMARY This paper focuses on optical integration technology and its application in optical microsensors used in biomedical fields. The integration is based on the hybrid integration approach, achieving high performance, small size and weight, and lower cost. First, we describe the key technologies used in hybrid integration, namely passive alignment technology, low temperature bonding technology, and packaging technology for realizing advanced microsensors. Then, we describe an integrated laser Doppler flowmeter that can monitor blood flow in human skin.

key words: *microsensors, hybrid integration, passive alignment, low temperature bonding, laser Doppler flowmetry*

1. Introduction

Optical sensors have proved to be essential in many industrial and medical applications due to various reasons, such as high sensitivity and advantages with non-invasive sensing. Conventional optical sensors are generally produced by assembly procedures based on three-dimensional alignment of bulk optical components. However, reducing the size of the components for miniaturization makes the components more difficult to align.

An optical integration approach is expected to solve this problem. Both monolithic [1]–[5] and hybrid [6]–[12] approaches can be used for integration of optical devices. Monolithic integration, where all required components are manufactured simultaneously on a single substrate, is the lowest cost approach for integration if high yields can be achieved. However, the yield of monolithic components reduces as process complexity increases. Hybrid integration of materially different components made with wide ranges of processes onto a single platform enables us to construct highly functional, reliable, and low-cost optical devices, such as optical telecommunication modules [6], [7] and microsensors [8]–[12]. For example, Fig. 1 shows a high-resolution microencoder that can measure displacement or revolution angle [10]. In this microencoder, a laser diode (LD), photodiodes (PDs), and a Si micrograting are flip-chip bonded on a micromachined Si optical bench ($3 \times 2\,\mathrm{mm}^2$). Small encoders that can be moved at high speed and tucked into small spaces have great potential for many industrial applications that require highly precise motion control.

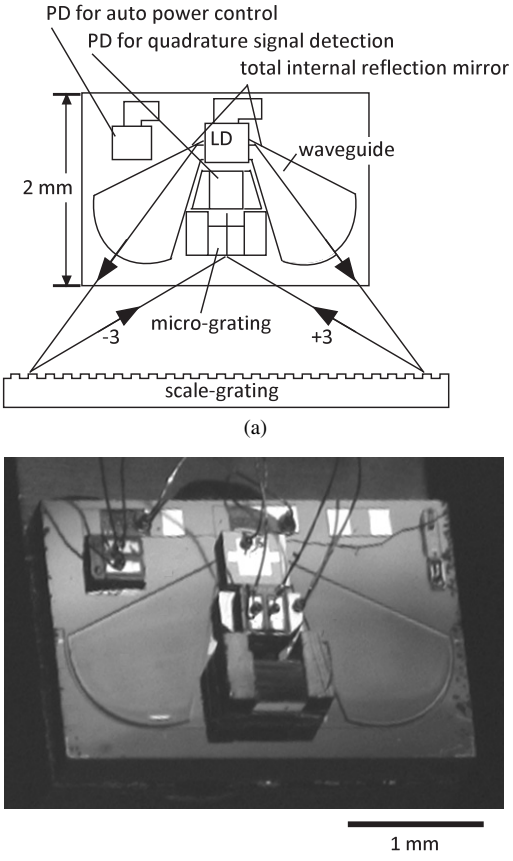

Fig. 1 Microencoder based on higher-order diffracted light interference. (a) schematic diagram, (b) photograph of the fabricated microencoder.

This paper will begin with a description of the optical integration technology required for the manufacture of an optical sensor system. In Sect. 2, we describe the key technologies used in hybrid integration: passive alignment technology, low temperature bonding technology, and packaging technology. In Sect. 3, we discuss the application of the micro-sensor in biomedical fields. We confirm the potential of hybrid integration technology by using it to fabricate an integrated laser Doppler flowmeter that can monitor blood flow in tissue.

Manuscript received July 12, 2008.
Manuscript revised October 21, 2008.

[†]The authors are with The University of Tokyo, Tokyo, 153-8904 Japan.
[††]The author is with Kyushu University, Fukuoka-shi, 819-0395 Japan.
a) E-mail: eiji@su.t.u-tokyo.ac.jp

DOI: 10.1587/transele.E92.C.231

2. Key Technologies

2.1 Passive Alignment Technology

The method of assembling optical devices is an important issue in relation to optical hybrid integration. Both active and passive alignment techniques have been developed. The active alignment technique is accomplished by the closed-loop optimization of the components position until the optimum of transmitted light is determined. In general, the equipment cost of the active alignment technique is very high and the processing time is relatively long. Therefore, the active alignment process becomes rather expensive and the throughput is quite low.

The passive alignment technique, which eliminates complicated precise optical axis alignment and removes the need for closed-loop optimization, can solve this problem. Three types of passive alignment techniques have already been developed: mechanical contact alignment [13], visual index alignment using alignment marks [7], [14], and solder bump self-alignment [15]. We adopted index alignment using alignment marks for hybrid integration [16]. This technique enables us to integrate optical active devices such as a LD and a PD with optical passive devices such as a waveguide and a grating on a Si substrate, which functions as both an optical bench and a heat sink. Integration of all components on a single Si platform results in considerable miniaturization. Combining high-performance chips allows highly reliable and multi-function devices.

Figure 2 illustrates the passive alignment technique. Prior to integration, a silicon terrace, Au/Pt/Ti (from top to bottom) electrodes and alignment marks, an eutectic AuSn solder layer, and a polyimide waveguide were formed on the silicon substrate. The silicon terrace for mounting the LD was fabricated by anisotropic etching in KOH solution. Au/Pt/Ti alignment marks were formed on both the LD and the silicon substrate. The laser beam was directly coupled to the polyimide waveguide without lens systems. The polyimide waveguide has a slab structure comprised of three layers: a lower cladding, a core, and upper cladding. The polyimide waveguide was fabricated by spin coating, curing at 370°C, conventional photolithographic patterning, and oxygen reactive ion etching with a silicone-based positive photoresist used as an etching mask. During the alignment, the LD is held active-layer-down (junction-down). The alignment in the vertical direction [Fig. 2(a)] is carried out simply by placing the LD chip on the solder layer, because the position of the waveguide core center is designed to be identical to the position of the active layer of the LD. The alignment in the horizontal direction is carried out using alignment marks [Fig. 2(b)]. The marks on both the LD and the silicon substrate are simultaneously observed using infrared light and an auto-focusing method [16], or inserting the two-sight camera unit between the LD and silicon substrate. By matching the alignment marks, the LD chip is aligned in the horizontal direction to the substrate plane. The bonding accuracy is usually better than $\pm 1\ \mu$m.

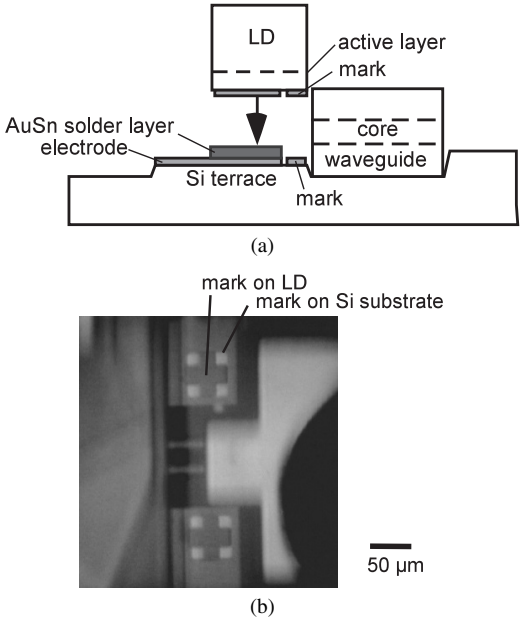

Fig. 2 Passive alignment technique using alignment marks. (a) cross-sectional view (schematic diagram), (b) top view (photograph).

2.2 Low Temperature Bonding Technology for Advanced Microsensor

In the hybrid integration process, eutectic AuSn (80–20 wt%) has commonly been used for optoelectronic applications (melting temperature: 280°C) because the AuSn has a very high yield strength and is typically free from thermal fatigue and creep movement, in addition to its excellent heat conduction properties. However, the AuSn bonding process has the following disadvantages:

1) Lack of plastic deformation of the AuSn results in its inability to release stresses, which may cause the chip to crack.
2) The AuSn bonding process requires a temperature above 300°C to ensure complete melting and this high temperature processing degrades temperature-sensitive materials (i.e. polymer). It also causes cracking or debonding of chips made of electro-optical materials having a large coefficient of thermal expansion (CTE) mismatches with the substrate (for example, the CTE for $LiNbO_3$ is $7.5 - 14.4 \times 10^{-6}\ K^{-1}$, whereas the CTE for Si is $2.6 \times 10^{-6}\ K^{-1}$) because of the thermal stress at the bonding interface during the heating and cooling processes [17].
3) It is essential to develop a multi-chip assembly technique for highly functional devices. However, the high thermal conductivity of the Si makes it difficult to perform local heating of the solder. When the AuSn is repeatedly melted, the Sn in the AuSn becomes oxidized. This is the main cause of difficulty in producing a perfect bond.

4) Most active optical components, such as LD and PD, require hermetic encapsulation in order to fulfill their requirements for performance, operation stability, and long lifetime. Here, the soldering temperature for hermetic encapsulation must be well below the AuSn melting temperature used to bond the chips. However, soft solder for low-temperature soldering is subject to significant creep deformation.
5) The AuSn has very steep liquidus lines on both sides of the eutectic melting point (280°C). For example, enriching the eutectic composition by 1 wt% of Au leads to an approximately 30°C increase in the melting temperature [18]. This suggests that the AuSn solder system requires very accurate process control of both the solder composition and the bonding temperature.

Considering these properties, there is great demand for a low-temperature and solderless bonding process to produce more highly functional optical devices. We have demonstrated low temperature bonding of a LD on a Si substrate using surface activation of Au by radio-frequency (RF) plasma irradiation [19]. Surface-activated bonding is a direct bonding method that joins two clean surfaces using the adhesive force of surface atoms at room temperature or low temperature. The clean surfaces are prepared by a dry process, such as ion beam bombardment. Since Au does not form surface oxides, it has been demonstrated that surface activation will work well for the bonding of Au in ambient air.

Surface-activated flip-chip bonding tests were conducted using commercially-available GaAs vertical-cavity surface-emitting laser (VCSEL) chips with 600-nm-thick Au electrodes and Si substrates with 500-nm-thick Au electrodes. The bonding was carried out on the n-electrode side of the VCSEL chip. A terrace structure was fabricated on the Si substrate to avoid any effects on the bonding by the edge of the VCSEL. The contact area between bonded samples was $240\,\mu\text{m} \times 240\,\mu\text{m}$.

The bonder is composed of a pretreatment chamber for plasma cleaning and a bonding chamber for alignment and bonding. The bonding process was performed according to the following procedure. 1) The organic contaminations on the Au surfaces of the VCSEL chip and the Si substrate are removed by an Ar RF plasma in the pretreatment chamber. The etching rate for Au film is about 30 nm/min (plasma power: 100 W). 2) The VCSEL chip and Si substrate are transferred into the bonding chamber for alignment and bonding. The bonding is carried out by contact in ambient air. Static pressure is applied to the chip during heating, with the chip kept at the peak temperature for 30 s.

Figure 3 shows the flip-chip bonded VCSEL with the n-side down on the terrace. Bonding was carried out in air at low temperature (bonding temperature: 150°C, contact load: 900 gf) after the Au surfaces of the VCSEL and the Si substrate were cleaned by an Ar RF plasma (plasma irradiation time: 150 s, plasma power: 100 W). We performed die-shear tests according to MIL-STD-883G, Method-2019

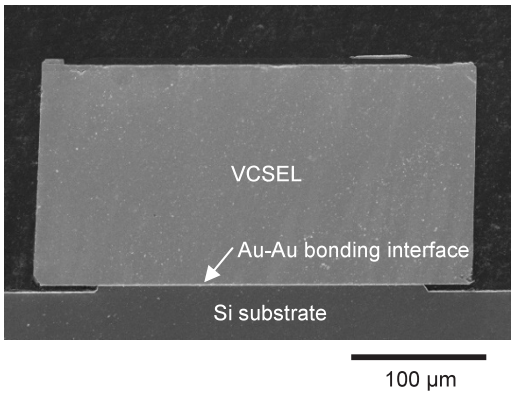

Fig. 3 Typical cross-sectional SEM images of bonded VCSEL on Si substrate by Au-Au surface-activated bonding (bonding temperature: 150°C, contact load: 900 gf).

[20] in order to evaluate the bonding strength. The minimum force (1.0 ×) to pass the test for a $300\,\mu\text{m} \times 300\,\mu\text{m}$ chip is 56 gf. Without plasma irradiation, die shear strength was approximately 0 gf. This means that the thermocompression bonding [21], [22] is not possible under this condition. When the plasma irradiation time was increased above 120 s, however, high die-shear strengths of over 120 gf were obtained.

The light-current-voltage (L-I-V) curves were evaluated to evaluate optoelectronic characteristics of bonded VCSELs. The measurement was performed by continuous wave operation. Figure 4(a) shows the typical L-I-V characteristics before and after surface-activated bonding (plasma irradiation time: 150 s, bonding temperature: 150°C, contact load: 900 gf). Compared with the unbound VCSEL, the bonded VCSEL showed almost the same characteristics for electrical and optical data. However, when the contact load was increased from 900 gf to 2500 gf, the threshold current, I_{th}, increased and the light output power decreased after bonding as shown in Fig. 4(b). When the bonding temperature was increased from 150°C to 330°C, the light output power also decreased a little after bonding as shown in Fig. 4(c). It can be concluded that bonding temperature and contact load are the most critical parameters that have influences on optoelectronic characteristics as well as bonding quality.

2.3 Packaging Technology

One of the factors stalling commercialization of microsensors is the packaging. Optical microsensor packages are often required to provide both optical and electrical access, hermeticity, mechanical strength, and long-term reliability. At present, metal packaging with hermetic seals is used frequently in microsensor packaging as shown in Fig. 5. There are several industry standard metal cans, for example the well-known TO (transistor outline) metal cans. TO metal cans are also commonly used to house optoelectronic components. Conventional TO metal cans include a generally cylindrical metal cap and a metal header, to which the metal

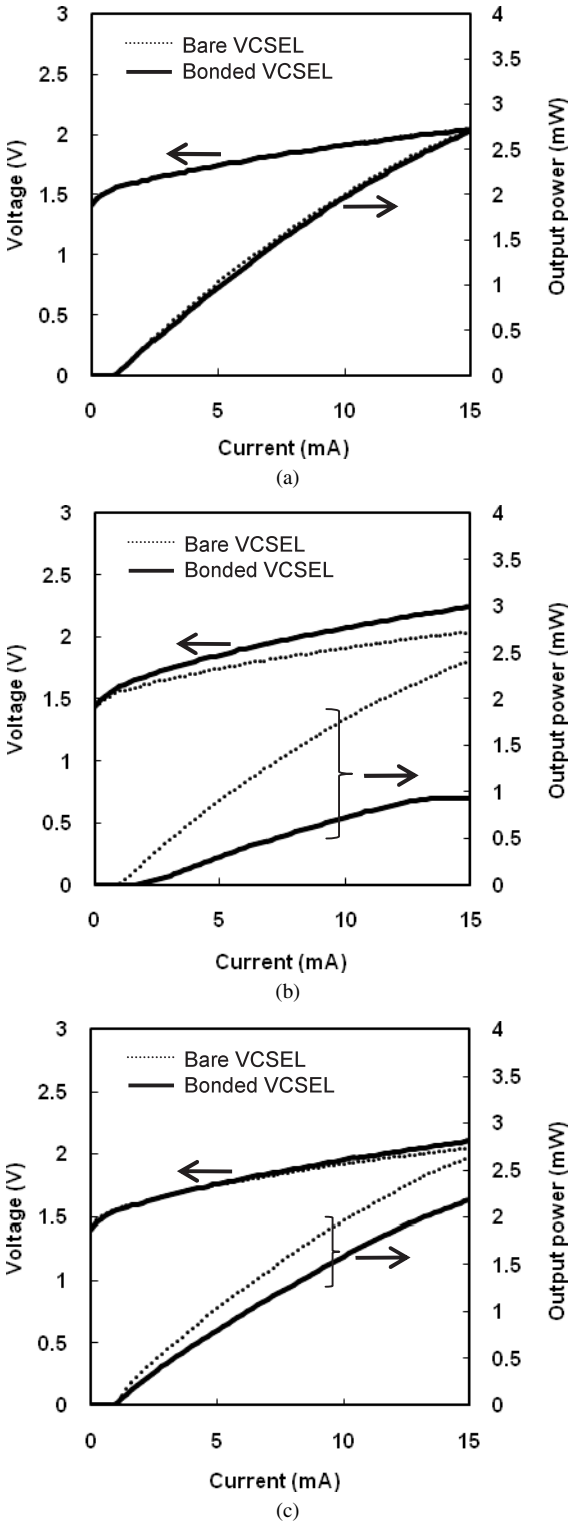

Fig. 4 L-I-V characteristics before and after surface-activated bonding. (a) plasma irradiation time: 150 s, bonding temperature: 150°C, contact load: 900 gf, (b) plasma irradiation time: 150 s, bonding temperature: 150°C, contact load: 2500 gf, (c) plasma irradiation time: 150 s, bonding temperature: 330°C, contact load: 900 gf.

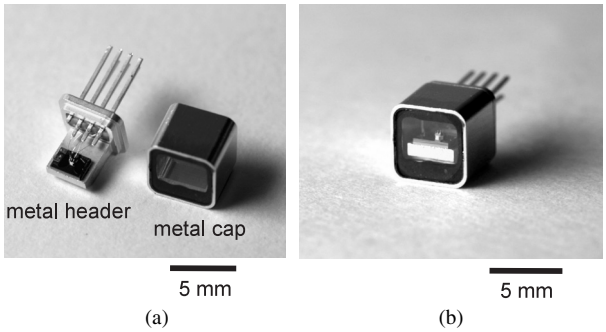

Fig. 5 Photographs of the metal-packaged microsensor. (a) before and (b) after seam welding.

cap is attached. In this package, metal-based bonding techniques such as, for example, brazing or laser welding, are often used to provide a hermetic seal between the metal cap and the header. There are disadvantages associated with the TO metal can. The fabrication process is expensive due to the need for a special mounting header and metal can and the size of the package is large. Also, expensive laser welding equipment has to be used when using the TO metal can. Accordingly, there is a need for an improved microsensor package assembly.

Wafer-level chip-scale packaging (WLCSP) has been a leading development in high-density electronic packaging. WLCSP combines the chip-scale package advantages of small size and ease of handling with an efficient volume production approach based on batch packaging processes that can fabricate a large number of packages simultaneously at the wafer level. The essence of WLCSP is that the packages are formed directly on the wafer, before the wafers are sawn and individual chips are separated.

Figure 6 shows the schematic configuration and photograph of the fabricated microsensor suitable for WLCSP. The size of the fully-integrated microsensor is 2.8 mm × 2.8 mm × 1 mm thick. It consists of two elements: 1) a micromachined Si optical bench incorporating a bonded LD, micromirrors, and through-hole electrodes; and 2) a glass substrate incorporating a bonded PD, electrical interconnection, and a refractive microlens. The top half of the microsystem package is a glass cap, which serves as an optical window with a microlens and a protective cover. The Si optical bench with a cavity defined by the {111} planes was used for free-space micro-optical bench. The laser beam is reflected by the ⟨111⟩ face of the cavity wall and then encounters the refractive microlens. After passing through the lens, the beam is collimated. To perform multi-chip integration, we adopted Au-Au surface-activated bonding. This bonding was used not only for optical chips such as a LD and a PD, but also to bond the glass substrate on the silicon optical bench. Currently, the two elements of the Si optical bench and the glass substrate are assembled after dicing the pieces individually. However, the design and fabrication process of this microsensor allow WLCSP.

When an optical microsensor chip and its associated

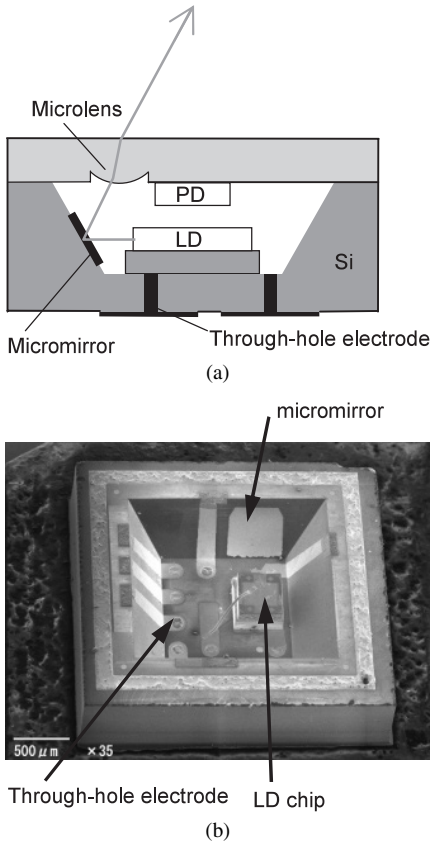

Fig. 6 Integrated microsensor suitable for wafer-level chip-scale packaging. (a) schematic configuration, (b) SEM photograph of the micromachined Si optical bench incorporating a bonded LD, micromirrors, and through-hole electrodes.

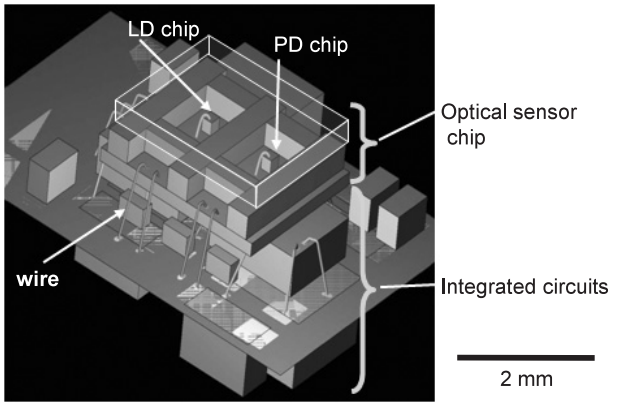

Fig. 7 Schematic diagram of the integrated laser Doppler flowmeter based on system-in-package (SiP) technology.

integrated circuits are spaced too far apart from each other, degradation of electrical signals occurs during transmission. Consequently, electrical performance may be improved when the distance between the microsensor chip and its associated integrated circuit chip is as short as possible. Integration of integrated circuits can be achieved either monolithically or in a hybrid fashion, leading to a system-on-chip (SoC) or a system-in-package (SiP) solution, respectively. SoCs, which are highly-integrated single-chip products, provide the lowest manufacturing cost, but design costs are often higher and development time and time-to-market is generally longer. SiPs allow integration of different kinds of multiple dies in a common package and offer a cost-effective alternative solution to SoC integration. Figure 7 shows the schematic diagram of the integrated laser Doppler blood flowmeter based on SiP technology [23]. In this structure, not just the optical chip (including a LD and a PD), but also integrated circuits such as operational amplifiers are successfully stacked in three layers.

3. Integrated Laser Doppler Flowmeter

Optical microsensors are also of great interest in biomedical applications because they are noninvasive. Miniaturized sensors can be used as wearable or implantable devices. Recently, wearable devices that gather physiological information continuously and noninvasively have been in high demand for long-term and wireless monitoring in hospitals and sport physiology. Several wearable devices in finger-ring [24] or wristwatch configurations have been developed. However, the incorporated sensors are restricted to either pulse-wave types or pulse oximeters containing light-emitting diodes [24], [25]. In these applications, it is most important that the sensors be small and light so that they can be worn comfortably.

Blood flow monitors have been of special interest for many years because they offer a promising tool for the noninvasive examination of the physiological state of the microcirculation. Impaired blood circulation is a major factor in the etiologies of many adult diseases. The first application of laser Doppler velocimetry to blood flow was reported by Riva et al. [26]. In 1975, Stern demonstrated that scattered light from laser-illuminated skin is Doppler broadened and that the Doppler width correlates with blood flow [27]. There are a number of ways to implement blood flowmetry and some of those have been put into clinical use. The most common technique involves the use of optical fibers to conduct the He-Ne laser light or laser diode (LD) light to the skin tissue and from the tissue to a photodetector [28]. However, the instrument requires positioning and alignment of individual optical components (such as lens and fiber) in three dimensions. As a result, the whole instrument becomes bulky with dimensions of tens of centimeters, although the probes are small. Such a large and heavy instrument is not suitable as a wearable device. Furthermore, movement or vibration of the fiber affects the output signal [29].

We have developed the first prototype of an integrated laser Doppler blood flowmeter that permits real-time monitoring of capillary microcirculation in tissue for a wearable monitoring system that can connect to communication networks [8]. The hybrid integrated structure includes an InGaAsP/InP distributed feedback laser diode (DFB LD) with a wavelength of 1310 nm, an edge-illuminated PD and a polyimide waveguide on Si substrate (2 mm × 3 mm)

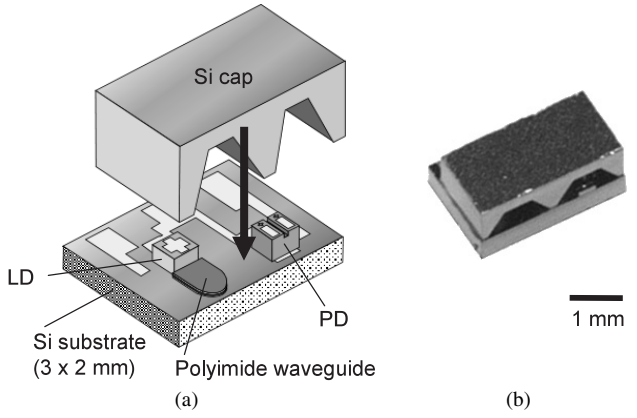

Fig. 8 Integrated laser Doppler flowmeter. (a) schematic diagram, (b) photograph.

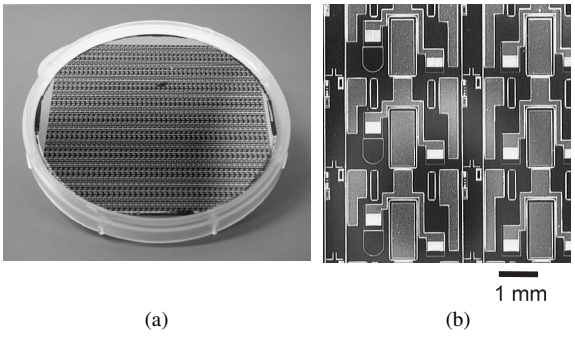

Fig. 9 Photographs of microfabricated Si substrate for integrated laser Doppler flowmeter. (a) 4 inch wafer, (b) enlarged view.

(Fig. 8). The Si substrate was fabricated by forming Si terraces, Au/Pt/Ti electrodes, AuSn solder layers, and three-layer polyimide waveguides using batch process technology as shown in Fig. 9. This flowmeter avoids the use of optical fibers and related motion artifacts. Figure 10 shows a blood flow measuring system using a PDA (Personal Digital Assistant) and Bluetooth technology. The sensor chip is mounted together with a hybrid integrated circuit which contains a pre-amplifier, and they are packaged as a compact sensor probe only $12 \times 21 \times 5.4$ mm in size. This sensor probe can be positioned directly on the tissue. The blood flow is derived by a digital signal processor in a quantitative (although relative) fashion in real time [8]. The blood flow signal can be plotted and displayed on a PDA screen or stored in a memory card. It is also possible to transmit the signal in wireless mode using Bluetooth technology.

We performed some measurements of blood perfusion from the fingertips of some volunteers. Figure 11 shows the power spectra of photocurrent from a fingertip. The upper spectrum was measured during normal perfusion and the lower during an occlusion of the upper arm with a pressurized cuff. There is clearly a distinct difference in the two frequency spectra. *In-vivo* measurements of blood perfusion in a fingertip confirm the feasibility of the blood flowmeter. The signal was in agreement with that obtained by a commercially available fiber-optic laser Doppler flowmeter.

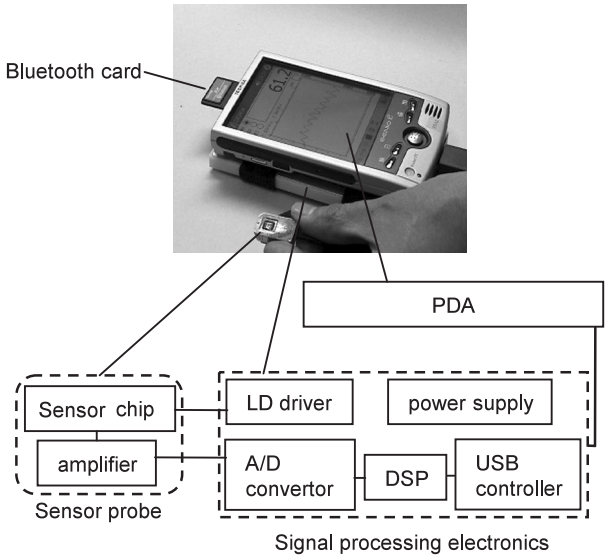

Fig. 10 Blood flow measuring system using a PDA (Personal Digital Assistant) and Bluetooth technology.

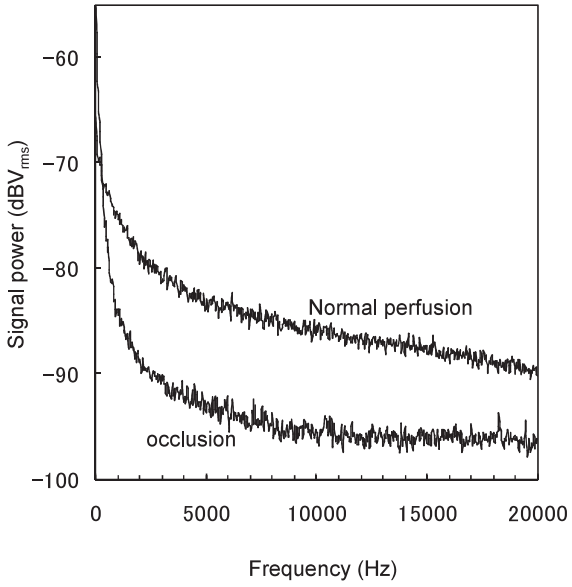

Fig. 11 The power spectrum of photocurrent from the fingertip. The upper arm was occluded with a pressurized cuff.

Figure 12 shows an example of the simultaneous recording of applied pressure and blood flow when a finger is pressed against the probe surface. The flow signal shows variations with pulsation. As the pressure applied to the finger gradually increased, the relative intensity of blood flow decreased due to poor circulation. The amplitude of pulsation is considered to be at maximum when the applied pressure is made to equalize the intraarterial pressure in the finger.

4. Conclusions

This paper reported the key technologies necessary for hybrid integration and its application for optical microsensors

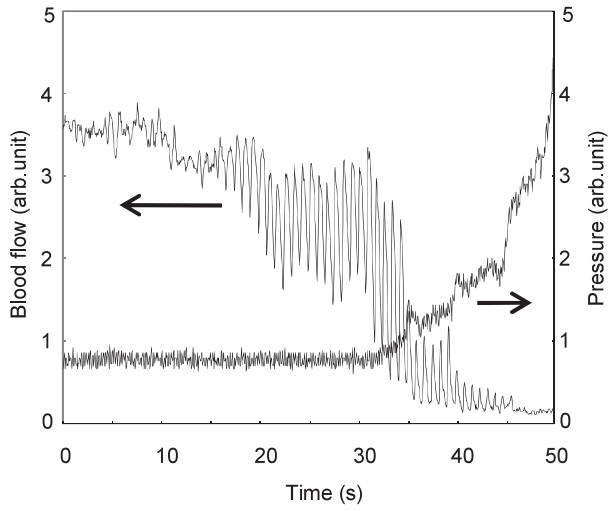

Fig. 12 Simultaneous recording of applied pressure and blood flow when a fingertip is pressed against the sensor probe surface.

in use in biomedical fields. The hybrid integration of various optical microcomponents by passive alignment and low temperature bonding has opened up many new possibilities in constructing highly functional, reliable, and low-cost optical microsensors. In addition, wafer-level chip-scale packaging provides a way to enable the system-in-package (SiP) type of ultra compact and thin packaging of hybrid integrating optoelectronics and signal processing circuits together. Using these technologies, a highly miniaturized, simply constructed laser Doppler flowmeter has been successfully developed. This integrated probe avoided the use of optical fibers and related motion artifacts. These optical microsensors seem to be promising for realizing future wearable or implantable devices in the biomedical application field.

Acknowledgments

A part of this study was supported by Industrial Technology Research Grant Program in 2006 from New Energy and Industrial Technology Development Organization (NEDO) of Japan. A part of this work was carried out at NTT.

References

[1] R. Sawada, E. Higurashi, T. Ito, O. Ohguchi, and M. Tsubamoto, "Monolithic-integrated micro-laser encoder," Appl. Opt., vol.38, no.33, pp.6866–6873, Nov. 1999.

[2] E. Higurashi, R. Sawada, and T. Ito, "Monolithically integrated optical displacement sensor based on triangulation and optical beam deflection," Appl. Opt., vol.38, no.9, pp.1746–1751, March 1999.

[3] T. Ito, R. Sawada, and E. Higurashi, "Integrated micro laser Doppler velocimeter," J. Lightwave Technol., vol.17, no.1, pp.30–34, Jan. 1999.

[4] R. Sawada, E. Higurashi, and T. Ito, "Integrated microlaser displacement sensor," J. Micromech. Microeng., vol.12, pp.286–290, April 2002.

[5] T. Ito, R. Sawada, and E. Higurashi, "Integrated micro-displacement sensor that uses beam divergence," J. Micromech. Microeng., vol.13, pp.942–947, Aug. 2003.

[6] Y. Yamada, S. Suzuki, K. Moriwaki, Y. Hibino, Y. Tohmori, Y. Akatsu, Y. Nakasuga, T. Hashimoto, H. Terui, M. Yanagisawa, Y. Inoue, Y. Akahori, and R. Nagase, "Application of planar lightwave circuit platform to hybrid integrated optical WDM transmitter/receiver module," Electron. Lett., vol.31, pp.1366–1367, Aug. 1995.

[7] T. Hashimoto, Y. Nakasuga, Y. Yamada, H. Terui, M. Yanagisawa, Y. Akahori, Y. Tohmori, K. Kato, and Y. Suzuki, "Multichip optical hybrid integration technique with planar lightwave circuit platform," J. Lightwave Technol., vol.16, no.7, pp.1249–1258, July 1998.

[8] E. Higurashi, R. Sawada, and T. Ito, "An Integrated laser blood flowmeter," J. Lightwave Technol., vol.21, no.3, pp.591–595, March 2003.

[9] R. Sawada, E. Higurashi, and Y. Jin, "Hybrid microlaser encoder," J. Lightwave Technol., vol.21, no.3, pp.815–820, March 2003.

[10] E. Higurashi and R. Sawada, "Micro-encoder based on higher-order diffracted light interference," J. Micromech. Microeng., vol.15, pp.1459–1465, June 2005.

[11] R. Sawada, E. Higurashi, T. Ito, and I. Ishikawa, "An accelerometer incorporating a laser microencoder for a wide measurable range," Sensors and Actuators A, vol.136, no.1, pp.161–167, May 2007.

[12] I. Ishikawa, R. Sawada, E. Higurashi, S. Sanada, and D. Chino, "Integrated micro-displacement sensor that measures tilting angle and linear movement of an external mirror," Sensors and Actuators A, vol.138, no.2, pp.269–275, Aug. 2007.

[13] E.E. L. Friedrich, M.G. Oberg, B. Broberg, S. Nilson, and S. Valette, "Hybrid integration of semiconductor lasers with Si-based single-mode ridge waveguide," J. Lightwave Technol., vol.10, no.3, pp.336–340, March 1992.

[14] M.S. Cohen, M.J. DeFranza, F.J. Canora, M.F. Cina, R.A. Rand, and P.D. Hoh, "Improvements in index alignment method foe laser fiber array packages," IEEE Trans. Compon. Hybrids. Manuf. Technol., vol.17, no.3, pp.402–411, Aug. 1994.

[15] J. Sasaki, M. Itoh, T. Tamanuki, H. Hatakeyama, S. Kitamura, T. Shimoda, and T. Kato, "Multiple-chip precise self-aligned assembly for hybrid integrated optical modules using Au-Sn solder bumps," IEEE Trans. Adv. Packag., vol.24, no.4, pp.569–575, Nov. 2001.

[16] R. Sawada, E. Higurashi, and T. Ito, "High accurate and quick bonding of a laser-diode chip onto a planar lightwave circuit," Prec. Eng., vol.25, no.4, pp.293–300, Oct. 2001.

[17] R. Takigawa, E. Higurashi, T. Suga, S. Shinada, and T. Kawanishi, "Low-temperature Au-to-Au bonding for $LiNbO_3$/Si structure achieved in ambient air," IEICE Trans. Electron., vol.E90-C, no.1, pp.145–146, Jan. 2007.

[18] C.H. Lee, Y.M. Wong, C. Doherty, K.L. Tai, E. Lane, D.D. Bacon, F. Baiocchi, and A. Katz, "Study of Ni as a barrier metal in AuSn soldering application for laser chip/submount assembly," J. Appl. Phys., vol.72, no.8, pp.3808–3815, Oct. 1992.

[19] E. Higurashi, T. Imamura, T. Suga, and R. Sawada, "Low temperature bonding of laser diode chips on Si substrates using plasma activation of Au films," IEEE Photonics Technol. Lett., vol.19, no.24, pp.1994–1996, Dec. 2007.

[20] United States Department of Defense, MIL-STD-883G, Test Method Standard, Microcircuits, Method 2019.7, Feb. 2006.

[21] J.L. Joppe and A.J.T. de Krijger, "Hybrid integration of laser diode and monomode high contrast slab waveguide," Electron. Lett., vol.27, no.2, pp.162–163, Jan. 1991.

[22] A. Ambrosy, H. Richter, J. Hehmann, and D. Ferling, "Silicon motherboards for multichannel optical modules," IEEE Trans. Compon. Packag. Manuf. Technol. A, vol.19, no.1, pp.34–40, March 1996.

[23] R. Seto, Y. Sawae, E. Higurashi, T. Itoh, T. Masuda, K. Suzuki, K. Tukamoto, T. Ikehara, R. Maeda, T. Fujitsu, and R. Sawada, "Micro-optical blood flow sensor based on system in package (SiP) technology that fuses optical MEMS and intergrated circuit to detect avian influenza," Synthesis and Reactivity in Inorganic, Metal-Organic, and Nano-Metal Chemistry, vol.38, no.3, pp.256–259, 2008.

[24] H.H. Asada, P. Shaltis, A. Reisner, S. Rhee, and R.C. Hutchinson, "Mobile monitoring with wearable photoplethysmographic biosensors," IEEE Eng. Med. Biol. Mag., vol.22, no.3, pp.28–40, May/June 2003.
[25] T. Torfs, V. Leonov, and R.J.M. Vullers, "Pulse oximeter fully powered by human body heat," Sensors & Transducers J., vol.80, no.6, pp.1230–1238, June 2007.
[26] C. Riva, B. Ross, and G.B. Benedek, "Laser-Doppler measurements of blood flow in capillary tubes and retinal arteries," Invest. Opthalmol., vol.11, pp.936–944, 1972.
[27] M.D. Stern, "In vivo evaluation of microcirculation by coherent light scattering," Nature, vol.254, pp.56–58, March 1975.
[28] D. Watkins and G.A. Holloway, Jr, "An instrument to measure cutaneous blood flow using the Doppler shift of laser light," IEEE Trans. Biomed. Eng., vol.BME-25, no.1, pp.28–33, Jan. 1978.
[29] T.P. Newson, A. Obeid, R.S. Wolton, D. Boggett, and P. Rolfe, "Laser Doppler velocimetry: The problem of fiber movement artefact," J. Biomed. Eng., vol.9, pp.169–172, April 1987.

Eiji Higurashi received an M.E. degree from Tohoku University in 1991. In that year, he joined the Applied Electronics Laboratories of NTT. He received his Ph.D. from Tohoku University in 1999. He has been an associate professor in the Department of Precision Engineering at the University of Tokyo since 2003 and an associate professor in the Research Center for Advanced Science and Technology (RCAST) at the University of Tokyo since 2004. He has been engaged in research on the integration and packaging of optical microsystems. He has received several awards, including the Igarashi Award in 2002, the Okawa Publications Prize in 2003, and the Ichimura Prize in 2008. He is a member of the Japan Society for Precision Engineering, the Japan Institute of Electronics Packaging, the Japan Society of Applied Physics, and a senior member of the Institute of Electrical Engineers of Japan.

Renshi Sawada received his B.E., M.E., and Ph.D. degrees from Kyushu University, Fukuoka-shi, Japan, in 1976, 1978, and 1995 respectively. In 1978, he joined the Electrical Communication Laboratories, NTT, Tokyo, Japan. He has been engaged in research on the polishing of Si substrates, the gettering of Si crystalline defects, and the fabrication of dielectrically isolated Si substrates (SOI substrate process), and optical MEMS such as micromirror arrays, integrated optical displacement sensors, integrated optical blood-flow sensors, integrated scanning microscopes, and sensors attachable to animals and humans for networking. Since January 2004, he has been working at Kyushu University, Fukuoka, Japan. He has received awards from the Japan Society of Precision Engineering in 1981 and 1991, the Okawa Publications Prize in 2003, and the ninth MOC paper prize in 2003. He has also served on the program committees of many conferences, is a fellow of the Institute of Physics, and is editor of the Journal of Micromechanics and Microengineering.

Tadatomo Suga received his Ph.D. from the University of Stuttgart in 1983, while performing his Ph.D. research at the Max-Planck Institute für Metallforschung, Stuttgart. In 1984, he became a member of the Faculty of Engineering, University of Tokyo, and since 1993, he has been a professor in the School of Engineering. He is also a chair of the IEEE CPMT Society Japan Chapter. His research focuses on microsystems integration and packaging and the development of interconnection technology, especially room-temperature bonding techniques for 3D integration. He has also advocated for the importance of the environmental aspects of packaging technology and is well known as the key organizer of the Japanese roadmap for lead-free soldering and the International Eco-design Conference.